Materials Today: Proceedings 45 (2021) 7228–7238

Contents lists available at ScienceDirect

Materials Today: Proceedings

journal homepage: www.elsevier.com/locate/matpr

Aerodynamic simulation of optimized vortex generators and rear spoiler for performance vehicles

M Palanivendhan [a,*], J Chandradass [a], Praveen Kumar Bannaravuri [b], Jennifer Philip [a], Kumar Shubham [a]

[a] Center for Automotive Materials, Department of Automobile Engineering, College of Engineering and Technology, SRM Institute of Science and Technology, Kattankulathur, Kanchipuram 603203, Tamil Nadu, India
[b] Department of Mechanical Engineering, Karunya Institute of Technology and Science, Coimbatore 641114, Tamil Nadu, India

ARTICLE INFO

Article history:
Received 8 December 2020
Received in revised form 14 February 2021
Accepted 17 February 2021
Available online 20 March 2021

Keywords:
Car model
Drag
Vortex generator
Wind tunnel

ABSTRACT

In today's world, where fuel prices in all modes of transport are skyrocketing, car manufacturers must find better and innovative ways to make their cars more energy efficient. A reduction in fuel consumption of a vehicle directly corresponds to the non- renewable fossil fuels' lesser consumption and a decrease in vehicular pollution. All road vehicles under driving conditions are made to pass through a wall of air around them and displace this air envelope as efficiently as they can depend upon the vehicle's shape and frontal area. As it flows around the car, this air envelope is responsible for drag force, which is the main opposition to the vehicle's forward motion. This drag force is proportional to the square of the velocity of the car and as a result, increases significantly after certain speeds. In most passenger vehicles due to constraints created by cabin space, regulations, etc., the cars end up being somewhat obliquely and boxy shaped, leading to turbulence, particularly towards the rear end of the car. This formation of turbulence results in flow separation at a point near the vehicle's rear windshield, which causes the boundary layer to not adhere to the body surface, expand and create a high-pressure region which induces drag along this portion of the vehicle. When placed at the specific distance upstream of the flow separation point, the vortex generators play a pivotal role in reducing drag and lift. And coupled with a rear wing can give suitable downforce values and drag reduction by redirecting the flow of air at the right angle of approach to the wing and preventing flow separation. The drag reduction is obtained by changing the angle of attack of the airstream with the wing by changing the orientation of vortex generators.

Selection and peer-review under responsibility of the scientific committee of the International Conference on Mechanical, Electronics and Computer Engineering 2020: Materials Science.

1. Introduction

The drag is a force that acts parallel to the airflow and along the direction of it. The way a vehicle behaves as it travels through the air is dependent on its coefficient of drag. A major factor on which this drag coefficient would depend on would be the vehicle body's shape. This aerodynamic drag is critical at higher speeds as it increases with the speed's square. It is beneficial to reduce the drag coefficient to improve vehicle performance parameters such as handling, acceleration, vehicle top speed, and fuel efficiency. A vortex generators' primary function would be to energize the air in the boundary layer and delay separation. This device is typically used in critical flow areas. They appear as small wing objects installed at an angle of 90° onto a surface/body at variable angles of attack. Each vortex generator is set at an angle of attack. The vortex generator develops vortex at its tip; the base is approximately parallel to the surface on which the device is mounted. The vortices induced by the vortex generator tend to combine the airflow in the boundary layer with the high-pressure free-stream air. The process energizes the slow boundary layer air. It delays the turbulence causing flow separation process to an increased distance behind the car's roofline, as shown in this study. The effect produced due to the combined effect of the rear wing and vortex generators has not been adequately studied yet and much is to be achieved in this field by using vortex generators with varying angle of attack to achieve desired aerodynamic performance characteristics. The reduction in drag is seen to improve the fuel economy of the vehicle. The fuel economy's improvement resulting from employing such a VG in combination with the spoiler is also calcu-

* Corresponding author.
E-mail address: palanivm@srmist.edu.in (M Palanivendhan).

https://doi.org/10.1016/j.matpr.2021.02.537
2214-7853/
Selection and peer-review under responsibility of the scientific committee of the International Conference on Mechanical, Electronics and Computer Engineering 2020: Materials Science.

lated and documented. The vortex generator's orientation and shape play a vital role in controlling the amount of drag reduction. In previous research papers, studies on different orientations of vortex generator and its effect on the aerodynamic drag is seen. Here we use a designed VG installed at different orientations on the vehicle that has a pre-installed spoiler. The best orientation of the VG on the vehicle is determined for most drag reduction. The result is seen to vary with the rake angle of the VG. The designed VG is altered for different rake angles, and the differences in drag reduction are determined. M. Williams et al. [1] demonstrated an authentication of a CFD code in order to exemplify the capability of swift multi-body regeneration under similar topological conditions. Md. Rasedul Islam et al. [2] put forth a research in order to show the effect of delayed separation of flow on the roof at the downstream side by means of a vortex from the rear-end of the roof as used in aircrafts to prevent the same. Mohan Jagadeesh Kumar et al. [3] explained how the main reason for the aerodynamic drag in a car is the flow separation from its rear end and how it could be reduced by means of a vortex generator having a bump-shaped module. P. Gopal et al. [4] studied the various parameters present in an utility vehicle such as coefficient of drag, dynamic pressure with and without the presence of vortex generators at changeable yaw angles. Fazalul Rahman et al. [5] illustrated the how the vortex generators effect the changes in the flow separation at fluctuating orientation to the flow field. Joseph Katz et al. [6] demonstrated how making modifications in the aerodynamics of sports cars could reduce the downforce of the vehicle. L. Anantha Raman et al. [7] deliberated how various methods of reducing aerodynamic drag therefore bringing about a decrease in the fuel consumption of the vehicles. S. M. Rakibul Hassan et al. [8] analyzed the aerodynamic drag experienced in race cars and solved for the drag coefficient by Finite Volume Method. K. Karthik et al. [9] assessed the aerodynamic drag and various other aspects of a cylindrical module by employing LES and provided a particle swarm optimization technique for the issue of drag. Zulfaa Mohammed-Kassim et al. [10] analyzed how fuel economy could be achieved by means of devices that could help in drag reduction for heavy vehicles. Kobayashi et al. [11] provided a detailed study predicting the reduction in drag effect by means of pulsating turbulent flow. Vignesh Ram et al. [12] used a wall-mounted cylindrical protrusion in order to understand the outcome of using vortex generators on the field of flow at variable Mach Numbers. Jae Sung Yang et al. [13] designed and developed a dimpled cooling channel in order to carry out numerical simulations by means of a vortex generator in order to determine the best value for thermo-aerodynamic performance. Vigneshwaran et al. [14] proposed an improved free-vortex method in order to compute the aerodynamics from the HAWT's blades under conditions of pitching and yawing. Hobeika et al. [15] tested a new methodology using different simulations of tyre in order to understand its effects on the aerodynamics of passenger cars. The following research work was conducted by taking key points from the aforementioned prominent works.

2. Experimental setup

2.1. Wind tunnel testing

Wind tunnels are tube-like chambers with air passing through the inside of the tube consisting of an inlet and outlet. It is used in automobiles to determine the aerodynamic forces (i.e., drag, downforce). Here in work, we are using subsonic wind tunnel testing in our wind tunnel the maximum speed is 72 km/hr that speed is enough to calculate the air velocity and pressures for a scaled-down model of the vehicle undergoing aerodynamic study. Bernoulli's principle can be used to determine the air's velocity that would pass through the test section of the wind tunnel. Measurements of the dynamic pressure and the rise of temperature in the test section airflow. Tufts of yarn are used to identify the direction of the flow of air around the car model. Threads mounted in the test section ahead of and after the test model are used to visualize the direction of the airflow approaching the test model surface. Bubbles or smoke are introduced along the model to determine the flow characteristics. Beam balances are used to measure aerodynamic forces associated with the test model. Small holes are drilled into the test model throughout the airflow path's length and using multiple tubes manometer the probe point pressures are measured. The pressure distribution over the test model is determined by this method.

3. Methodology

3.1. Modelling of vortex generator

We are using Creo 5.0 software for modelling. Modelling VG with different attack angles says 20, 25 and 30 and the optimum angle is taken and that VG is attached to the car model. The length, height and thickness of all vortex generators are in the same range with slight variations in dimensions. The length of the VG is approx. 50 mm, the height is 25 mm, and the thickness is 6.25 mm. In regions where the surface transitions are greater than 12°, vortex generators, diffusers are used to cut up the airflow. The idea is that areas like the transition between the hood and roof or roof and rear windshield on the average automobile create a large vortex. Vortex generators work on the principle of delaying flow separation at the back of the vehicle by deliberately inducing vortices in the airflow in the wake of the car. These vortices have a low-pressure region in their centre which causes the column of high-pressure air moving above it to get sucked into the vortex thereby keeping the flow attached, minimizing turbulence and resulting drag.

3.2. CAD design

The vortex generators are made as part files and attached at equal distances on the roof of the vehicle in Creo using the Assembly feature as shown in Fig. 1. They are assembled equidistant and perpendicular to the roof of the car at the point of attachment. The number of VGs was kept at six for optimum drag reduction, referring available research.

3.3. Star CCM+

The complete CFD analysis was carried out in Star CCM + software which is the industry standard for performing such applica-

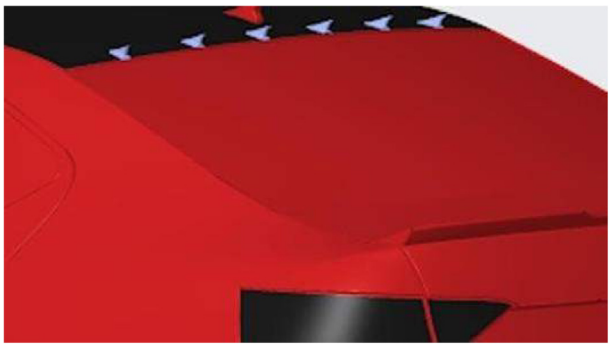

Fig. 1. Vg on Car model.

tions. The following steps were performed in said software to obtain final result.

3.4. Creation of flow domain

The CAD was imported in IGS format into the software and the flow domain (wind tunnel) was created around the vehicle in Star CCM + whose dimensions are as follows:

1. Length = 30 m
2. Breadth = 12 m
3. Height = 7 m

Given below in Fig. 2 is the wind tunnel (flow domain/ fluid medium) snapshot enclosing the vehicle body as shown. The car body is placed in the front half of the wind tunnel around 3 m in front of the half line along the x-axis. It is placed centrally along the z-axis and the wheels touch the ground of the wind tunnel with respect to the y-axis. The marker dimensions for vehicle placement in the wind tunnel are as follows:

3.5. Meshing

Next, we generate the mesh in the software. The meshing models used were trimmer, prism layer mesher, surface remesher and surface wrapper. The base cell size for the given wind tunnel dimensions was selected to be 0.3 m with a maximum cell size of 700% base size. Volumetric control was used to keep the cell size down near the vehicle body to around 9% of base size while cell size was more significant near the inlet, outlet, sides and floor of the wind tunnel. The number of prism layers on the vehicle body was restricted to two to keep the cell count down resulting in a volume mesh consisting of around 1035000–1100000 cells as shown in Fig. 3.

Similar inputs were given for generating volume mesh for all the Vortex Generator iterations to obtain optimized mesh and cut down on computing time. Given below is a snapshot of a plane along the car's length to visualize the volume mesh being generated. As we can see above the cells is kept coarse near the inlet, outlet and sides where fine cells are not required. This is an effective method of visualizing the mesh topology beforehand. Given below in Fig. 4, is a 3d representation of wrapper mesh on the vehicle body with Vortex generators attached to the roof.

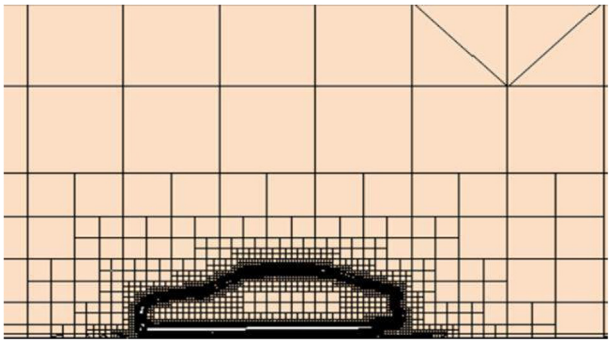

Fig. 3. Mesh of the Vehicle body.

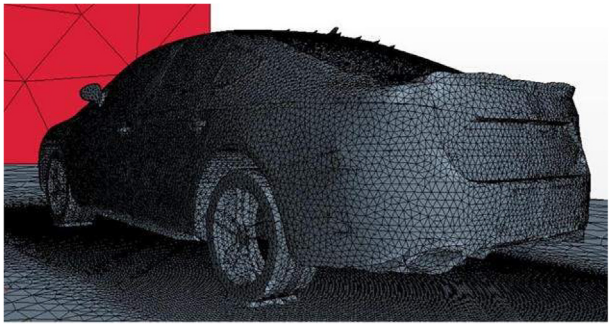

Fig. 4. 3D mesh of the Vehicle body.

3.6. CFD analysis

Computational Fluid Dynamics (CFD) uses numerical methods and algorithms to solve problems based on fluid flow. It is a simulation of the interaction between gases and liquids with a test surface defined by BC.

The following physics parameters were kept constant for CFD analysis of all the iterations:

- Inlet air velocity: 41.667 m/s (150 kmph)
- Pressure: 0 Pa
- Static Temperature: 300 K
- Turbulent Viscosity Ratio: 10

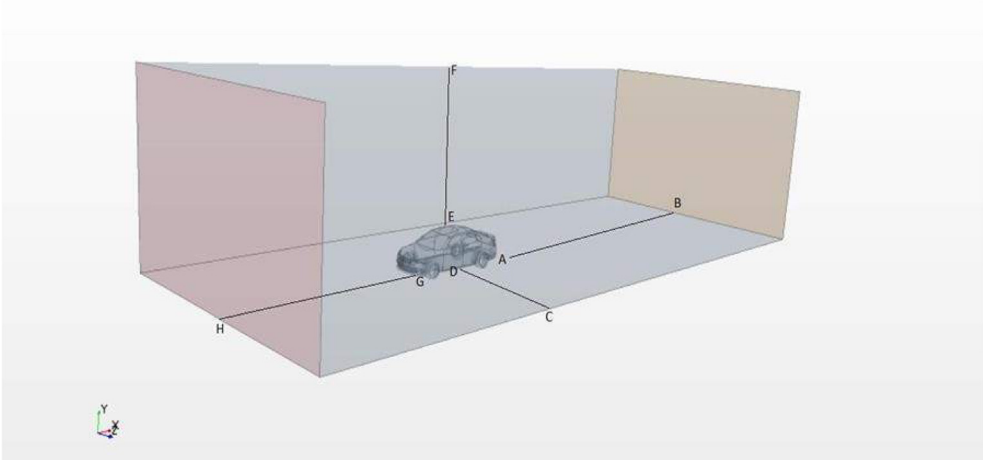

Fig. 2. Flow Domain. AB = 18 m DC = 6 m EF = 5.6 m GH = 8.5 m.

3.7. CFD analysis of car model without VG

We can see that the pressure distribution is higher than the model having VG, so there is no reduction in drag and lift forces. The pressure created on the roof is higher in a car model without VG. In this, if the pressure increases the velocity also decreases in the car model without VG. The flow separation is also high in this model because of a rise in pressure on the roof. Next, the scalar scene (output) was created to interpret the result of the CFD. Three planes were plotted along the vehicle body along all the three axes as shown in the figure to obtain the topology (distribution) of the following parameters on the planes:

- Total pressure distribution
- Velocity distribution

On the vehicle body itself, parameters like wall shear stress and pressure were also plotted as seen in the attached snapshots. A wind tunnel scene was also created with animation of streamlines around the vehicle body and pressure distribution throughout the wind tunnel.

3.8. Velocity distribution without VG

Fig. 5 shows the velocity profile distribution on a plane plotted along the car's length. Maximum velocity is attained on the vehicle's roof of around 42.683 m/s while the lowest velocity of around 0 m/s exists just behind the vehicle. As we can see without the vortex generators, there is a low-velocity region that extends quite long in the vehicle's wake that creates drag.

3.9. Total pressure distribution without VG

Fig. 6 shown below illustrates the total pressure distribution on a plane plotted along the car's length. As we can see, there is a low-pressure region created behind the vehicle for an extended length indicating turbulence. The maximum pressure is 765.76 Pa present all around the vehicle body and flow domain except on the rear windshield and wake of the car where minimum pressure of around 56 Pa exists.

3.10. Streamline inside wind tunnel without VG

Aforementioned Fig. 7, shows an isometric view of the flow domain and vehicle within streamlines being animated to show the vehicle's flow characteristics. The streamlines themselves show the velocity distribution with max velocity (37.217 m/s) above the vehicle's roof and around the sides and low velocity (24.821 m/s) in the wake. In contrast, the wind tunnel floor, inlet and outlet and vehicle body show the absolute pressure distribution and total pressure distribution, respectively.

3.11. Drag plot without VG

The drag plot monitor in Fig. 8 continuously plots the vehicle body's drag forces for the duration of all the iterations to complete (in this case 500), and the drag is measured at the second last (498th) iteration in all the cases given below. The x-axis plots the iteration number while the y-axis plots the drag force in Newton. In this case, drag without the VG attached = 952.607 N.

3.12. CFD analysis of car model with VG

Here we are running CFD for an angle of attack 20. The optimum angle of VG is taken for further process. We can see the angle 20 is optimum; by this angle, we are getting a maximum reduction of drag forces. The angle of attack in question is the one shown in Fig. 9.

3.13. VG at angle 20°

In this angle, the drag reduction and the flow separation reduction is high and was found out to be the most efficient angle of attack for the vortex generator. The drag reduction in this is 15%

3.14. Velocity distribution (Angle 20°)

Fig. 10 shows the velocity profile distribution on a plane plotted along the length of the car. Maximum velocity is attained on the roof near the front windshield of 53.688 m/s while the lowest velocity of 0 m/s exists just behind the vehicle. As we can see with the vortex generators at the angle of attack of 20°, a low-velocity region extends the shortest in the wake of the vehicle that creates drag, rendering this the most drag reduction iteration.

3.15. Total pressure distribution (Angle 20°)

Fig. 11 shows the total pressure distribution on a plane plotted along the length of the car. As we can see, there is a low-pressure region being created behind the vehicle for the shortest length as

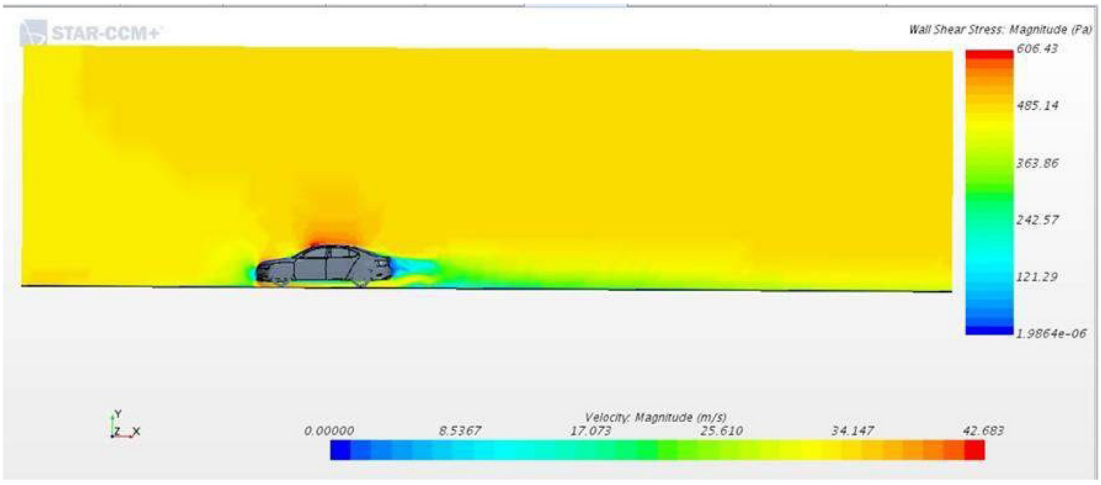

Fig. 5. Velocity profile distribution without VG.

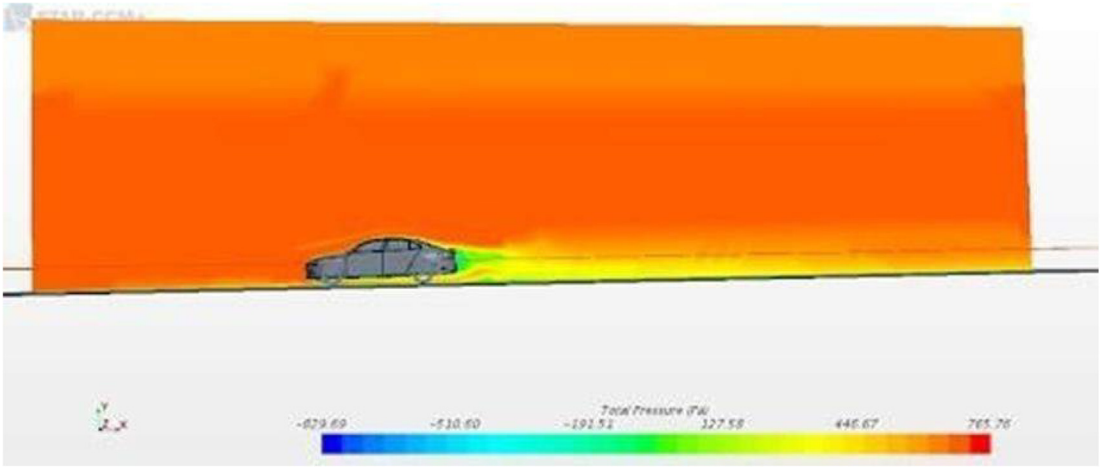

Fig. 6. Pressure distribution without VG.

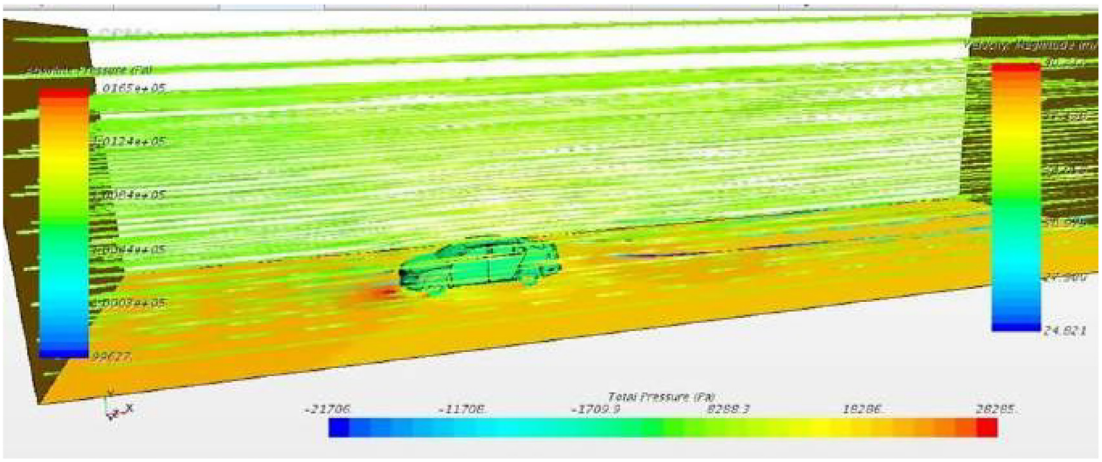

Fig. 7. Streamline inside wind tunnel without VG.

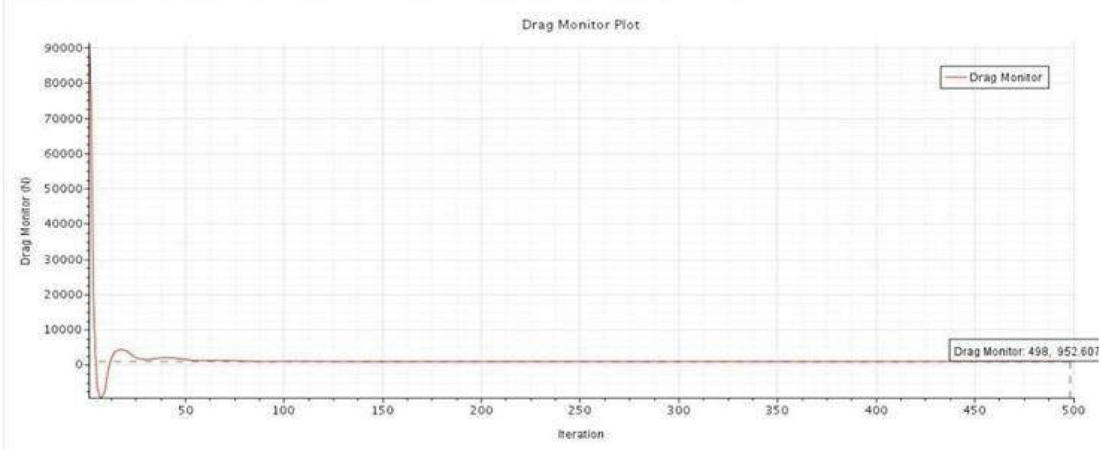

Fig. 8. Drag plot for without VG.

compared to the previous case indicating least turbulence, while on the car body itself, wall shear stress has been plotted which does not exceed 3 Pa. The maximum pressure is 1120 Pa present all around the vehicle body and flow domain except on the rear windshield and wake of the car where minimum pressure of around 100 Pa exists.

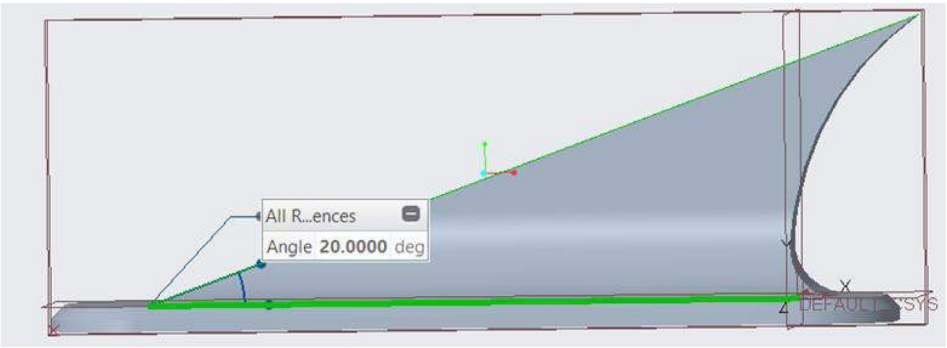

Fig. 9. Designed VG.

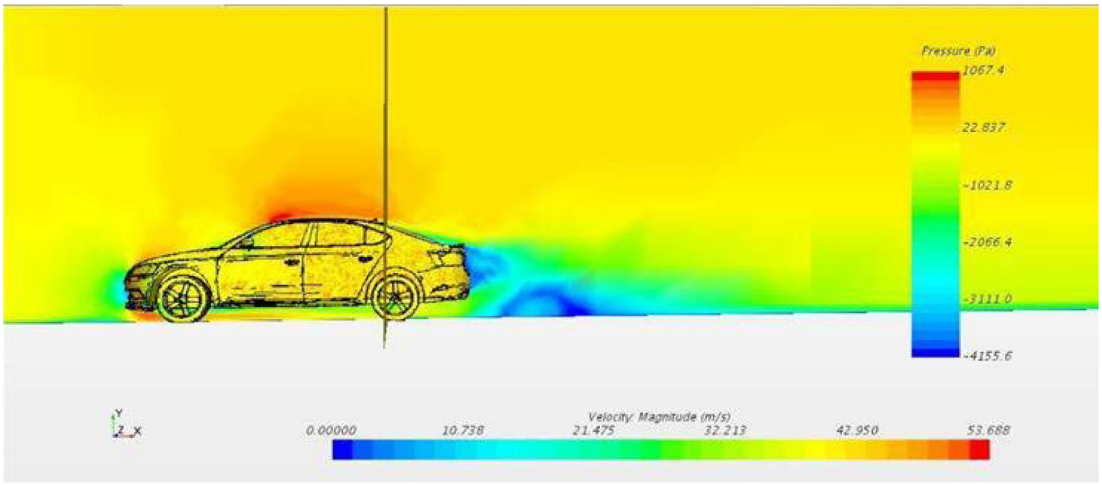

Fig. 10. Velocity profile distribution with VG (Angle 20°) View 1.

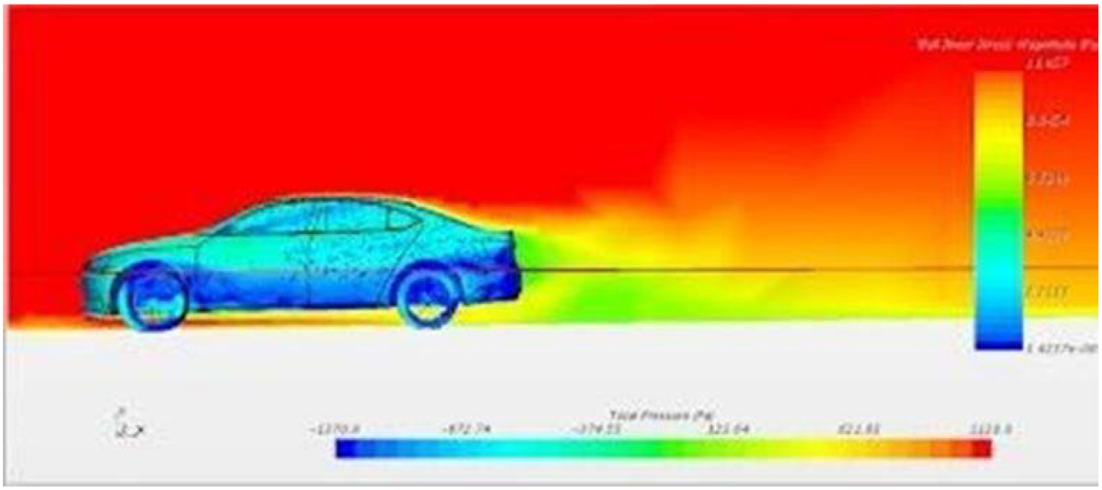

Fig. 11. Total Pressure distribution with VG with VG (Angle 20°) View 1.

3.16. Stream line inside wind tunnel (Angle 20°)

Fig. 12 shows an isometric view of the flow domain and vehicle within the streamlines being animated to show the vehicle's flow characteristics. The streamlines themselves show the velocity distribution with max velocity (47.724 m/s) above the vehicle's roof and around the sides and low velocity (32.832 m/s) in the wake while the wind tunnel floor, inlet and outlet and vehicle body show the total pressure distribution respectively.

3.17. Drag plot (Angle 20°)

The drag plot monitor shown in Fig. 13 continuously plots the vehicle body's drag forces for the duration of all the iterations to

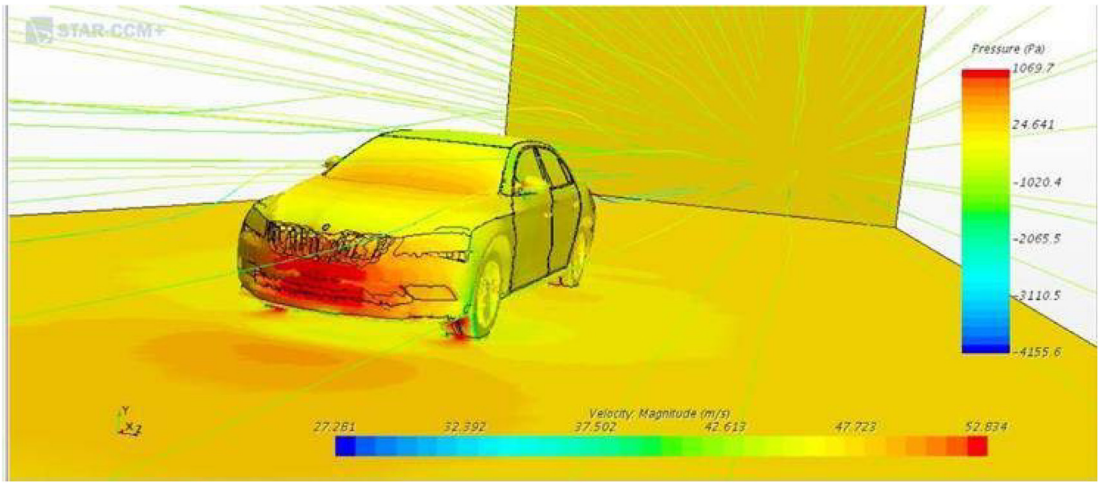

Fig. 12. Streamline inside wind tunnel with VG (Angle 20°)

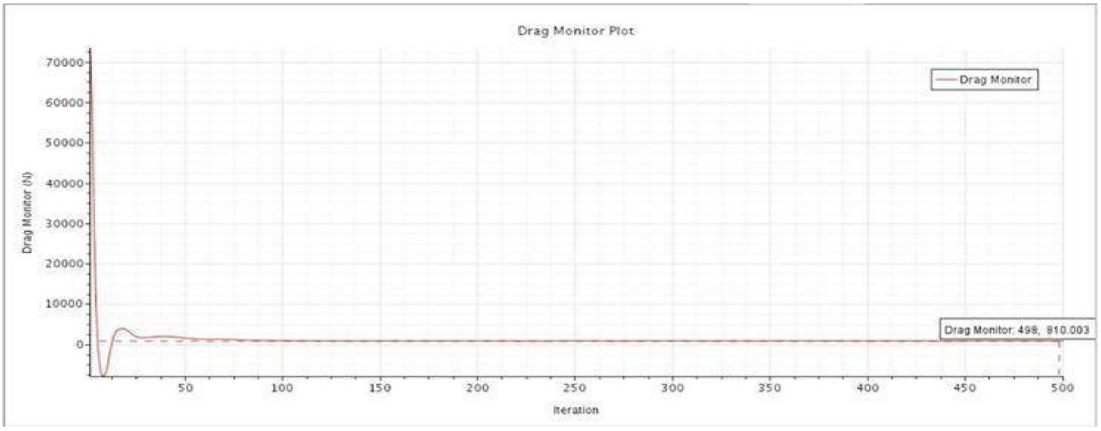

Fig. 13. Drag plot with VG (Angle 20°).

complete (in this case 500), and the drag is measured at the second last (498th) iteration in all the cases given below. The x-axis plots the iteration number while the y-axis plots the drag force in Newton. In this case,

Drag with VG attached (Angle 20°) = 810.003 N

3.18. CFD results for calculated wind speeds

In the previous calculations using a speed of 70 kmph were arrived upon based on a typical long-distance journey. This is where the main objective of the vortex generators may come into play by the reduction in drag forces acting upon the vehicle Here on, the vortex generators being used will be featuring an angle of attack of 20° as that was chosen to be the optimum angle with most drag reduction in this work.

3.19. Wind speed 70 kmph

The above wind speed was chosen for calculation because the wind tunnel available for the work (within college campus) has a maximum wind speed of around 70 kmph hence we chose to run the CFD for this wind speed for real-time comparison. We compare the improvement in aerodynamic characteristics of the vehicle by the following three parameters as given below, which are namely:

- Total Pressure Distribution
- Velocity Distribution
- Drag monitor plots

3.20. Total pressure distribution

3.20.1. Without vortex generator

Fig. 14 shows the total pressure distribution on a plane plotted along the length of the car. As we can see, there is a low-pressure region created behind the vehicle for an extended length indicating turbulence. The maximum pressure is 239.96 Pa present all around the vehicle body and flow domain except on the rear windshield and wake of the car where minimum pressure of around 20 Pa exists for an extended wake distance behind the car's back.

3.20.2. With vortex generator

Fig. 15 shows the total pressure distribution on a plane plotted along the length of the car. As we can see, there is a low-pressure region being created behind the vehicle for an extended length indicating turbulence, while the car body itself shows the plot of wall shear stress with maximum stress not exceeding 1 Pa. The maximum pressure is 243.95 Pa present all around the vehicle body and flow domain except on the rear windshield and wake of the car where minimum pressure of around 20 Pa exists for a reduced wake distance behind the back of the car due to the imple-

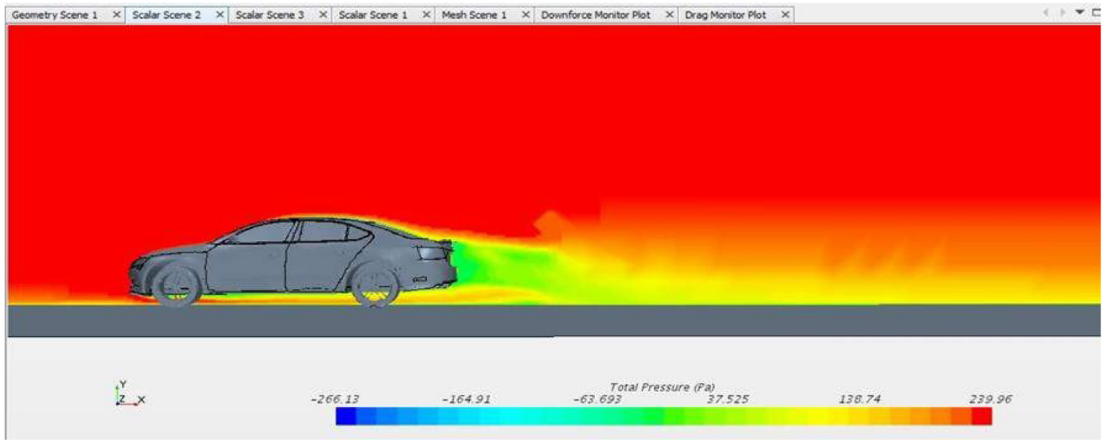

Fig. 14. Total pressure distribution without VG.

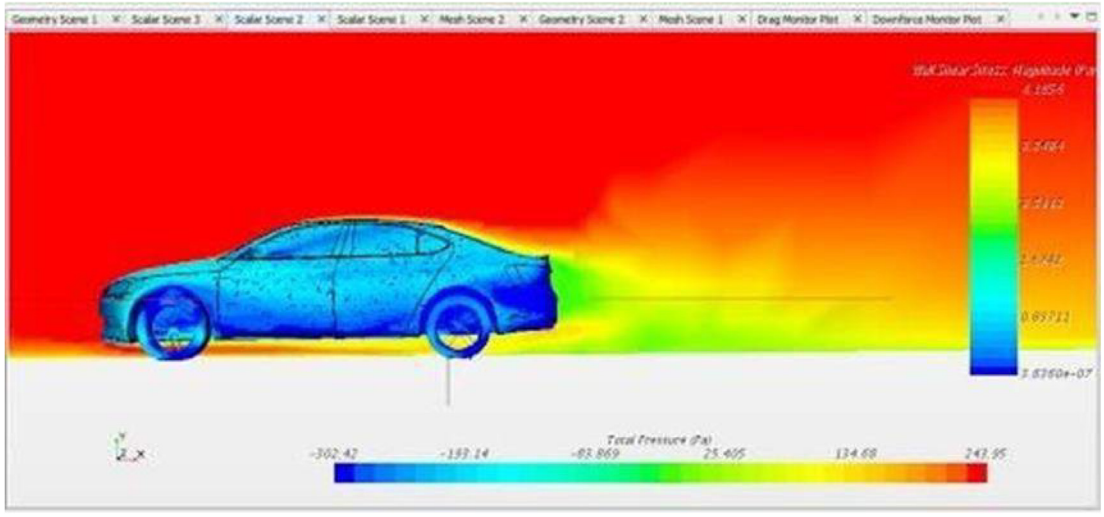

Fig. 15. Total pressure distribution with VG.

mentation of vortex generators of the optimum angle of attack as decided earlier.

3.21. Velocity distribution

3.21.1. Without vortex generator

The Fig. 16 shows the velocity profile distribution on a plane plotted along the length of the car. Maximum velocity attained on the roof near the front windshield of the vehicle of 24.874 m/s while the lowest velocity of 0 m/s exists just behind the vehicle. In contrast, the vehicle body itself shows the plot of wall shear stress with the maximum stress not exceeding 3 Pa. As we can see with the vortex generators, there is a low-velocity region that extends quite shorter in the wake of the vehicle that creates drag.

3.21.2. With vortex generator

Fig. 17 shows the velocity profile distribution on a plane plotted along the length of the car. Maximum velocity attained on the roof

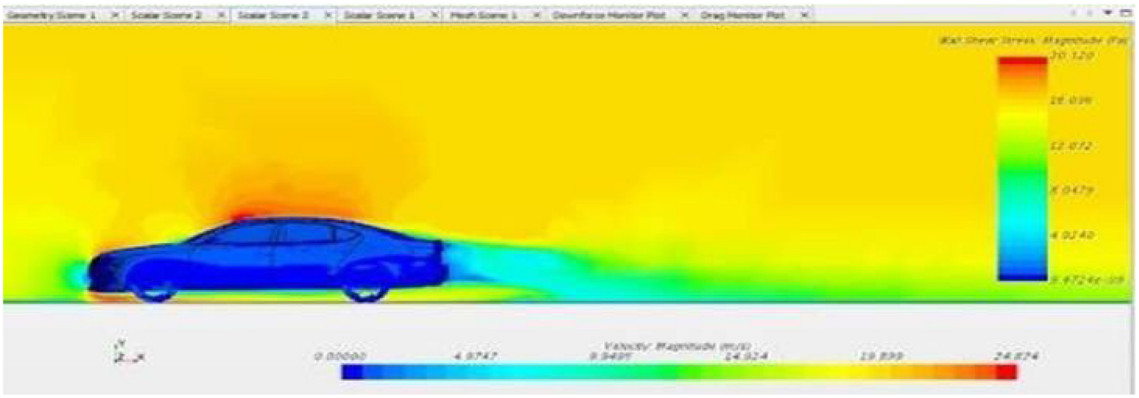

Fig. 16. Velocity Distribution without VG.

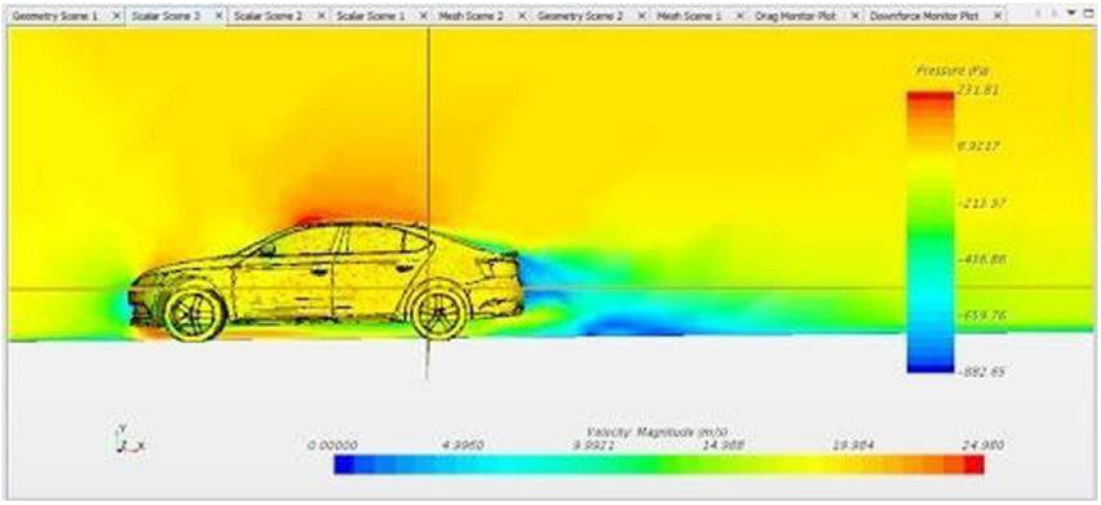

Fig. 17. Velocity Distribution with VG.

near the front windshield of the vehicle of 24.89 m/s while the lowest velocity of 0 m/s exists just behind the vehicle. As we can see with the vortex generators, there is a low-velocity region that extends a bit shorter in the vehicle's wake that reduces drag a bit even at this low speed.

3.22. Drag monitor plots

3.22.1. Without vortex generator

The drag plot monitor mentioned in Fig. 18 continuously plots the vehicle body's drag forces for the duration of all the iterations to complete (in this case 500), and the drag is measured at the second last (498th) iteration in all the cases given below. The x-axis plots the iteration number while the y-axis plots the drag force in Newton. In this case, we can see a drag of around 194.118 N obtained for the base model at a speed of 70 kmph.

3.22.2. With vortex generator

The drag plot shown in Fig. 19 monitors 5.5 continuously plots the vehicle body's drag forces for the duration of all the iterations to complete (in this case 500), and the drag is measured at the second last (498th) iteration in all the cases given below. The x-axis plots the iteration number while the y-axis plots the drag force in Newton. In this case, we can see drag of around 179.377 N is obtained for the model with vortex generators at a speed of 70 kmph.

3.23. Calculation

At the speed of 70 kmph, the drag force without and with vortex generators is 194.118 N and 179.377 N respectively, That gives us:

=179.377/194.118 = 0.924 Therefore 1–0.924 = 0.075*100
=7.5% reduction in drag at a speed of 70 kmph.

4. Wind tunnel validation

To obtain real-time validation of the results we got from CFD, we had to perform wind tunnel testing of the given model. This was carried out in the aerospace hangar of college premises, specifically the aerodynamics laboratory, equipped with a subsonic wind

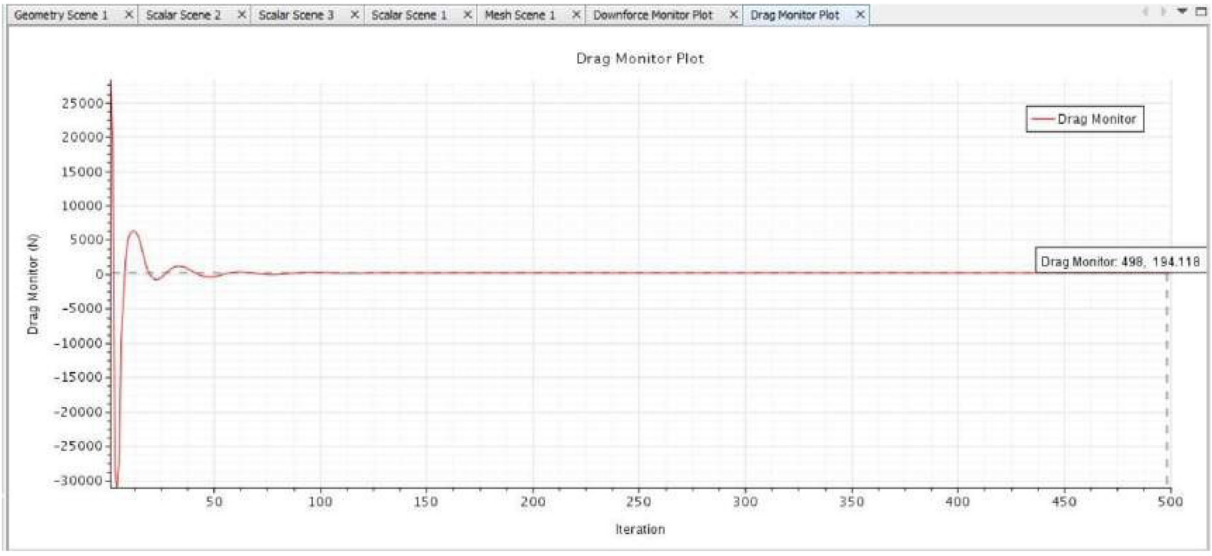

Fig. 18. Drag plot for without VG.

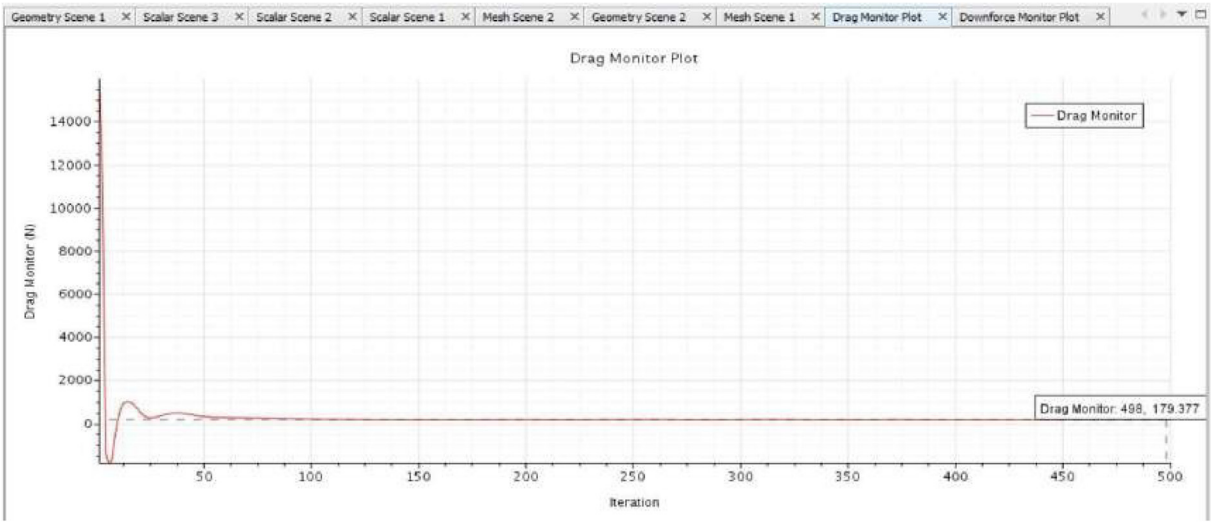

Fig. 19. Drag plot for with VG.

tunnel of maximum inlet velocity 20 m/s equivalent to 72 kmph. The specifications of the subsonic wind tunnel are as follows:

Blowdown type

This type of wind tunnel features a centrifugal type blower fitted upstream of the test section, unlike open-circuit tunnels which feature a fan assembly located downstream that sucks in the air using suction. This type of wind tunnel offers flexibility during different test conditions. The test bench cross-sectional area of the wind tunnel is 600 × 600 mm

This type of wind tunnel shown in Fig. 20 features a high-pressure area (reservoir) upstream of the test section and a low-pressure area downstream. The test starts with a high-pressure area upstream causing the medium (air) to flow downstream. This flow continues to flow to the low-pressure area that lies downstream until both regions' pressures have equalized. Once this happens, the pressure equalizes, and the test is over.

4.1. 3D models specifications

The 3D model was printed. The scaled-down model was not to exceed 10% of the test section cross-area hence for the model; we chose a scale down a factor of 1:31 to the real size model. The CAD model printed was that of the Octavia VRS with vortex generators having an angle of attack of 20° as decided to be the most optimum angle in the study conducted above. Since the model was small, a high degree of accuracy was required.

Fig. 20. Wind tunnel.

4.2. Procedure

Holes (number = 6) were drilled along the centreline of the model to insert the pressure pores. Pressure pores were created by inserting thin plastic tubes into the holes and connecting the pipes to a manometer mounted outside the test section. The manometer then gives the pressure distribution across the car body by comparing the pressure difference with the reference tubes. Once we calculate the drag coefficient, we can calculate drag at each pressure pore using the Drag force formula. The results are then compared with CFD to get real-time validation.

5. Conclusion

We are simulating the model for the vortex generator's different orientations, like changing the number of vortex generators, changing the angle of attack, placing the vortex generators in equal distance. The best-simulated orientation is taken to show that in real-time by using wind tunnel testing. The 3D printing of the selected car model with the best orientation will do wind tunnel testing. Wind tunnel gives the drag value along with flow characteristics. The results are 12 to 15% of drag reduction. The use for this drag reduction is that we have attained a saving in fuel consumption and showed the fuel consumption efficiency improvement according to the calculations.

Declaration of Competing Interest

The authors declare that they have no known competing financial interests or personal relationships that could have appeared to influence the work reported in this paper.

References

[1] M. Williams, A. Shires, "Validation of CFD for Racing Car Analysis and Design." SAE Technical Paper 2002-01-3349, 2002.
[2] Rasedul Islam, Md., Amzad Hossain, Md., Mohammad Mashud, Tanvir Ibny Gias, Md. "Drag Reduction of a Car by Using Vortex", International Journal of Scientific & Engineering Research, 2013 4(7).
[3] M.J. Kumar, M. Anoop Dubey, Shashank Chheniya, Amar Jadhav, Effect of vortex generators on aerodynamics of a Car: CFD analysis, Int. J. Innov. Eng. Technol. 2 (1) (2013).
[4] P. Gopal, T. Senthilkumar. "Aerodynamics Drag Reduction in a Passenger Vehicle Using Vortex Generator with Varying Yaw Angles." ARPN Journal of Engineering and Applied Sciences, 2012 7(9).

[5] Fazalul Rahman, Iswarya Thiyagarjan, The effect of orientation of vortex generators on aerodynamic drag reduction cars, Int. Ref. J. Eng. Sci. 4 (7) (2015) 13–20.
[6] Joseph Katz, Kevin P. Cain. "Rapid, Low-Cost, Aerodynamic Development of a High-Performance Sports Car" SAE Technical Papers 2011.
[7] L. Anantha Raman, H. Rahul Hari, Methods for reducing aerodynamic drag in vehicles and thus acquiring fuel economy, J. Adv. Eng. Res. 3 (1) (2016) 26–32.
[8] S.M. Rakibul Hassan, Toukir Islam, Md. Mohammad Ali, Quamrul Islam, Numerical study on aerodynamic drag reduction of racing cars, Procedia Eng. 90 (2014) 308–313.
[9] K. Karthik, M. Vishnu, S. Vengadesan, S.K. Bhattacharyya, Optimization of bluff bodies for aerodynamic drag and sound reduction using CFD analysis, J. Wind Eng. Ind. Aerodyn. 174 (2018) 133–140.
[10] Zulfaa Mohamed-Kassim, Antonio Filippone, Fuel savings on a heavy vehicle via aerodynamic drag reduction, Transp. Res. Part D: Transp. Environ. 15 (5) (2010) 275–284.
[11] W. Kobayashi, T. Shimura, A. Mitsuishi, A. Murata, K. Iwamoto, Prediction of the drag reduction effect of pulsating pipe flow based on machine learning, Int. J. Heat Fluid Flow 88 (2021).
[12] P.S. Vignesh Ram, S. Das, H.D. Kim, Influence of vortex generators on cylindrical protrusion aerodynamics at various Mach numbers, Aerospace Sci. Technol. 58 (2016) 267–274.
[13] J.S. Yang, M. Jeong, Y.G. Park, M.Y. Ha, Numerical study on the flow and heat transfer characteristics in a dimple cooling channel with a wedge-shaped vortex generator, Int. J. Heat Mass Transfer 136 (2019) 1064–1078.
[14] Vigneshwaran, K., Palanivendhan Murugadoss, and K. Gokul. "Extraction and characterization of microfibers obtained from banana waste", No. 2017-28-1987. SAE Technical Paper, 2017.
[15] T. Hobeika, L. Lofdahl, S. Sebben, Study of different tyre simulation methods and effects on passenger car aerodynamics, Int. Vehicle Aerodyn. Conf. (2014) 187–195.